LETTER

The chiral edge state and Majorana fermion in hole-doped $YBa_2Cu_3O_{7-\delta}$ mesoscopic strip

A Letters Journal Exploring the Frontiers of Physics

April 2018

EPL, **122** (2018) 17006 www.epljournal.org
doi: 10.1209/0295-5075/122/17006

The chiral edge state and Majorana fermion in hole-doped $YBa_2Cu_3O_{7-\delta}$ mesoscopic strip

Xiao-Peng Yang[1], Guo-Qiao Zha[1,2] and Shi-Ping Zhou[1,2(a)]

[1] *Department of Physics, Shanghai University - Shanghai 200444, China*
[2] *Shanghai Key Laboratory of High Temperature Superconductors, Shanghai University - Shanghai 200444, China*

received 19 February 2018; accepted in final form 16 May 2018
published online 8 June 2018

PACS 74.78.Na – Mesoscopic and nanoscale systems
PACS 74.20.-z – Theories and models of superconducting state

Abstract – Edge states of nontrivial topology are investigated by diagonalizing the tight-binding Hubbard model Hamiltonian for the copper-oxide superconductor YBCO strip in the presence of the Rashba spin-orbit interaction and the Zeeman field. It is found that chiral edge states may develop under appropriate spin-orbit coupling and the exchange field strengths. By defining the quasi-particle creation (annihilation) operators in terms of the obtained particle and hole functions, the zero-energy chiral edge states are proved to be the Majorana zero-energy modes on the opposite edges of the superconductor strip. Manipulations on the Majorana modes are promising by applying an external magnetic field normal to the strip plane. It is also showed that the chiral edge state and the Majorana fermions are more feasible in the underdoped samples. Moreover, domains distinguishing the *d*-wave pairings from the *s*-wave pairings are found, implying the coexistence of the *d*-wave and *s*-wave gaps for the underdoped YBCO samples.

Introduction. – Topological superconductors associated with Majorana fermions have attracted great interest [1,2]. Majorana fermions are particles that are equivalent to their antiparticles [3], which are non-Abelian and have a potential to construct the qubits and for quantum computations [4,5]. A variety of systems have been studied to realize the non-Abelian topological phase, such as the fractional quantum Hall system [6–9], the chiral *p*-wave superconductors [10–14] and fermionic cold-atom systems [15–17]. States of matter with exotic properties are expected when interactions having a different symmetry with respect to that of Hamiltonian systems had been invoked. For instance, the *p*-wave pairing state may develop when a Rashba spin-orbit coupling is involved into the Hamiltonian mode of an *s*-wave superconductor [18].

Since the discovery of copper-oxide high-temperature superconductors (HTS) in 1986 [19], extensive efforts have been attracted. Despite the origin of high-T_c superconductivity remains unsolved, the pairing symmetry is generally considered to be a *d*-wave pairing in HTS [20]. As well known, properties of quasi-particles are closely correlated with the bulk topology of the pairing states and the topology of the Fermi surface in a superconductor. The copper-oxide superconductors are perovskite compounds whose superconductivity and Fermi surface vary drastically with the electron or hole-doping level. For instance, the ground state of the normal phase goes from a strongly antiferromagnetic (AFM) phase at an extremely underdoping level to the pseudo-gap region at underdoping, to the so-called marginal Fermi liquid at around the optimum doping, and to a normal Fermi liquid at the overdoped region in the hole-doped Y $Ba_2Cu_3O_{7-\delta}$ superconductor. Then, when the superconducting phase develops as the temperature is below the superconducting critical temperature T_c, competitions between different orderings, *e.g.*, the *d*-wave pairings and antiferromagnetic ordering, will give rise to an intrinsic mechanism that would lead to conversions between states with different parity (P) symmetry possibly. Actually, the degeneracy at the gap-closing points of a *d*-wave superconductor can be lifted by an exchange field, $h * \sigma$ (with σ the Pauli matrix and h the exchange field strength). Consequently, Fermi wavelength mismatching between electrons with opposite spins occurs, allowing the coexistence of spin-singlet and spin-triplet pairing amplitudes. Furthermore, states with nontrivial topology are expected when the Rashba spin-orbit cou-

(a) E-mail: spzhou@shu.edu.cn (corresponding author)

pling that violates the spin-rotation symmetry is included.

In this paper, we study the properties of the ground state in the mesoscopic d-wave HTS in the presence of the exchange field and the spin-orbit coupling, illustrating that the zero-energy chiral edge mode is the Majorana bound state (MBS). We will start with the model description, move to the discussion and clarification on the self-consistent solutions for the model, and finish with a brief conclusion.

Model. – We consider an infinitely long YBCO superconducting strip in the y-direction, and with a finite width in the x-direction. The effective mean field Hamiltonian of the Hubbard model in the presence of the Rashba spin-orbit (SO) interaction and exchange field can be written as

$$\hat{H} = \hat{H}_0 + \hat{H}_{so}, \tag{1}$$

$$\begin{aligned}\hat{H}_0 = &-\sum_{\langle ij\rangle,\sigma} t_{ij} c^\dagger_{i\sigma} c_{j\sigma} + \sum_{i,\sigma}(Un_{i\bar{\sigma}} - \mu) c^\dagger_{i\sigma} c_{i\sigma} \\ &-h\sum_i (c^\dagger_{i\uparrow} c_{i\uparrow} - c^\dagger_{i\downarrow} c_{i\downarrow}) + \sum_{\langle ij\rangle}(\Delta_{ij} c^\dagger_{i\uparrow} c^\dagger_{j\downarrow} + \text{H.c.}),\end{aligned} \tag{2}$$

$$\begin{aligned}\hat{H}_{so} = V_{so}\sum_i [&(c^\dagger_{i\uparrow} c_{i+\vec{e}_x\downarrow} - c^\dagger_{i\downarrow} c_{i+\vec{e}_x\uparrow}) \\ &- i(c^\dagger_{i\uparrow} c_{i+\vec{e}_y\downarrow} + c^\dagger_{i\downarrow} c_{i+\vec{e}_y\uparrow}) + \text{H.c.}],\end{aligned} \tag{3}$$

where U is the on-site repulsion interaction and V is the nearest-neighbor attractive interaction. $c^\dagger_{i\sigma}(c_{i\sigma})$ is the creation (annihilation) operator for the electron with position i and spin σ, n is the particle number operator, μ is the chemical potential and h is the exchange field strength. The nearest-neighbor hopping integrals are expressed as $t_{ij} = \bar{t}\cdot\exp[i\pi/\phi_0 \int_{r_j}^{r_i} \vec{\mathbf{A}}(\mathbf{r})\cdot \mathrm{d}\vec{\mathbf{r}}]$. Here, $\phi_0 = hc/2e$ is the flux quantum. V_{so} is the SO coupling amplitude. $\vec{A}(r)$ is the vector potential with the form of $\vec{\mathbf{A}} = (B/2)(-y, x, 0)$ with B the applied magnetic field strength.

The Bogoliubov-de Gennes (BdG) equation in real space is [21]

$$\sum_j^N \begin{pmatrix} \mathcal{H}_{ij\uparrow} - h & V_1^{so} & 0 & \Delta_{ij} \\ V_2^{so} & \mathcal{H}_{ij\downarrow} + h & \Delta_{ij} & 0 \\ 0 & \Delta^*_{ij} & -\mathcal{H}^*_{ij\uparrow} + h & V_3^{so} \\ \Delta^*_{ij} & 0 & V_4^{so} & -\mathcal{H}^*_{ij\downarrow} - h \end{pmatrix} \times \begin{pmatrix} u^n_{j\uparrow} \\ u^n_{j\downarrow} \\ v^n_{j\uparrow} \\ v^n_{j\downarrow} \end{pmatrix} = \varepsilon_n \begin{pmatrix} u^n_{i\uparrow} \\ u^n_{i\downarrow} \\ v^n_{i\uparrow} \\ v^n_{i\downarrow} \end{pmatrix}. \tag{4}$$

By making use of the translation symmetry, we perform the Fourier transformation of the electron operator with respect to the variable y. The BdG equation (4) becomes

$$\sum_j^N \begin{pmatrix} \mathcal{H}_{ij\uparrow} - h & V_1^{so}(ky) & 0 & \Delta_{ij} \\ V_2^{so}(-ky) & \mathcal{H}_{ij\downarrow} + h & \Delta_{ij} & 0 \\ 0 & \Delta^*_{ij} & -\mathcal{H}^*_{ij\uparrow} + h & V_3^{so}(-ky) \\ \Delta^*_{ij} & 0 & V_4^{so}(ky) & -\mathcal{H}^*_{ij\downarrow} - h \end{pmatrix} \times \begin{pmatrix} u^n_{j\uparrow}(ky) \\ u^n_{j\downarrow}(-ky) \\ v^n_{j\uparrow}(-ky) \\ v^n_{j\downarrow}(ky) \end{pmatrix} = \varepsilon_n \begin{pmatrix} u^n_{i\uparrow}(ky) \\ u^n_{i\downarrow}(-ky) \\ v^n_{i\uparrow}(-ky) \\ v^n_{i\downarrow}(ky) \end{pmatrix}. \tag{5}$$

Here $\mathcal{H}_{ij\sigma} = -(1-\delta_{ij})t^\perp_{ij} + (Un_{i\bar{\sigma}} - \mu - 2t^\parallel_i\cos(ky))\delta_{ij}$, $\Delta_{ij} = (1-\delta_{ij})\Delta^\perp_{ij} + 2\cos(ky)\delta_{ij}\Delta^\parallel_{ij}$, $V_1^{so} = V_3^{so} = V_{so}(\delta_{i+1,j} - \delta_{i-1,j} - 2\sin(ky)\delta_{ij})$, $V_2^{so} = V_4^{so} = V_{so}(-\delta_{i+1,j} + \delta_{i-1,j} + 2\sin(ky)\delta_{ij})$,

The self-consistent conditions are

$$\begin{aligned}\langle n_{i\uparrow}\rangle = &\frac{1}{Ny}\sum_{n,ky} f(\varepsilon_n(ky))|u^n_{i\uparrow}(ky)|^2 \\ &+ (1 - f(\varepsilon_n(ky)))|v^n_{i\uparrow}(ky)|^2,\end{aligned} \tag{6}$$

$$\begin{aligned}\langle n_{i\downarrow}\rangle = &\frac{1}{Ny}\sum_{n,ky} f(\varepsilon_n(ky))|u^n_{i\downarrow}(ky)|^2 \\ &+ (1 - f(\varepsilon_n(ky)))|v^n_{i\downarrow}(ky)|^2,\end{aligned} \tag{7}$$

$$\begin{aligned}\Delta^\perp_{ij} = &\frac{1}{Ny}\sum_{n,ky}\frac{V}{4}\Big[(u^n_{i\uparrow}(ky)v^{n*}_{j\downarrow}(ky) + u^n_{j\downarrow}(ky)v^{n*}_{i\uparrow}(ky) \\ &+ u^n_{i\downarrow}(ky)v^{n*}_{j\uparrow}(ky) + u^n_{j\uparrow}(ky)v^{n*}_{i\downarrow}(ky))\tanh\left(\frac{\beta\varepsilon_n}{2}\right)\Big],\end{aligned} \tag{8}$$

$$\begin{aligned}\Delta^\parallel_{ij} = &\frac{1}{Ny}\sum_{n,ky}\frac{V}{2}\cos(ky)\Big[(u^n_{i\uparrow}(ky)v^{n*}_{i\downarrow}(ky) \\ &+ u^n_{i\downarrow}(ky)v^{n*}_{i\uparrow}(ky))\tanh\left(\frac{\beta\varepsilon_n}{2}\right)\Big].\end{aligned} \tag{9}$$

In our calculations, we take $t = a = 1$, and the self-consistent iteration continues until the difference in n and Δ between two consecutive iterations is less than 10^{-6}.

The MBSs in the chiral edge states. – We first study properties of the edge state in the absence of the external magnetic field by solving the BdG equation in the K-space. We discuss the effect of the exchange field on the excitation spectrum. The obtained excitation spectra are shown in fig. 1. Look at eq. (5), the up- and down-spin bands are degenerate when the exchange field strength h is zero. As shown in the left panel for $h = 0$, the degeneracy at the gap-closing points of the d-wave superconductor is protected by the parity symmetry, and the edge state is trivial. However, the energy spectrum changes significantly when an appropriate exchange field presents, *e.g.* the middle panel in fig. 1 for $h = 0.55$. The degeneracy at preexisting gap-closing points for $h = 0$ is lifted, yielding a fully gaped energy spectrum. Noticeably, a pair of new

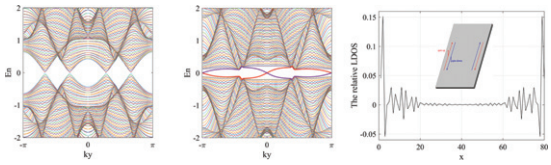

Fig. 1: (Color online) Energy spectra of the YBCO superconductor strip. Open boundary conditions in the x-direction and translation symmetry in the y-direction are assumed. The parameters used are $Nx = 80$, $Ny = 201$, $U = 3$, $V = 3$, $V_{so} = 1$, and $\bar{n} = 0.896$, but $h = 0$ (left panel) and $h = 0.55$ (middle panel). Right panel: the relative LDOS between up- and down-spin band. Inset: the schematic diagram of the chiral edge states.

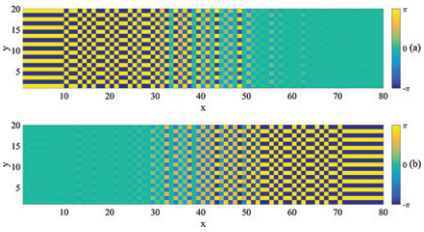

Fig. 2: (Color online) The phase difference between the particle and hole wave functions $u_\sigma(r)$ and $v_\sigma(r)$. (a) The up-spin band. (b) the down-spin band. The parameters are the same as in fig. 1, except that the periodic length of $Ny = 20$ is assumed.

edge states with a zero-energy crossing at $k = 0$ develops. The significance of the new zero-energy states lies in that they are stable against perturbations and are topologically protected, in contrast to the zero-energy modes for $h = 0$. There do exist gap nodes in our single-band (component) spin-singlet d-wave superconductor (left panel of fig. 1), and a V-shape local density of state spectrum is followed. Also, the gap closing is expected to occur at a vortex core, or strictly, the lowest core state has the energy scale Δ^2/E_F. However, the associated zero state is topologically trivial, particularly in that the relative phase between the quasi-particle and hole wave functions of those zero states does not have the relationship required for the Majorana zero-energy modes (see fig. 2 and discussions below). Actually, chiral edge states and a nonzero topological index are possible only when the Zeeman field and the Rashba spin-orbit coupling are introduced in the current case (middle panel of fig. 1). The relative local DOS between the up- and down-spin band is plotted in the right panel of fig. 1. It is seen that the zero-energy mode consists of a pair of chiral edge states. Namely, the up-spin electrons move along one direction and the down-spin electrons move in the opposite direction if an in-plane electric field is applied onto the sample. Therefore, while the electronic conductance is negligible a quantum spin-Hall current is expected. As shown in the middle and right panels (fig. 1) of our paper, chiral edge states are generated in the presence of an appropriated Zeeman field and Rashba spin-orbit interaction. The chiral edge states have the dispersion relations of $\mathrm{d}E(k)/\mathrm{d}k_y > 0$ (< 0) for the up (down)-electrons which implies that the up-spin electrons will move along the y-axis, while the down-spin ones move in the opposite direction at each of the strip borders. The equal amplitude but opposite direction electron flow in the opposite spin-band will lead to zero electric current $j_c = j_{i\uparrow} + j_{i\downarrow}$ when an electric field of y-direction is applied. On the contrary, a spin current if defined by $j_s = j_{i\uparrow} - j_{i\downarrow}$ is expected.

We emphasize that the characteristics of the zero-energy state depend strongly on the fermion parity or the lowest-energy state parity at the zero-energy crossing. There is a common consensus that the fermion parity is conserved in a closed superconductive system despite that the number of Cooper pairs may change. However, if fermions can create or destroy when the external parameter is tuned a situation may occur where the ground-state parity changes while crossing at zero energy. In this case on one side of the crossing the lowest-energy state has the even parity and on the other the odd parity state has the lowest energy. Therefore, one expects a sign reversing in the slope of the highest occupied bound state at the crossing. This means a reversing of the current and leads to a spin current jump, signaling a topological phase transition.

To clarify the zero-energy chiral edge state being the Majorana mode, we write down the Bogoliubov quasi-particle creation/annihilation operator ($\gamma_n^\dagger/\gamma_n$) as

$$\gamma_n^\dagger = \sum_i (u_{i\uparrow}^n c_{i\uparrow}^{n\dagger} - v_{i\downarrow}^n c_{i\downarrow}^{-n}) + (u_{i\downarrow}^n c_{i\downarrow}^{n\dagger} + v_{i\uparrow}^n c_{i\uparrow}^{-n}), \quad (10)$$

$$\gamma_n = \sum_i (u_{i\uparrow}^{n*} c_{i\uparrow}^n - v_{i\downarrow}^{n*} c_{i\downarrow}^{-n\dagger}) + (u_{i\downarrow}^{n*} c_{i\downarrow}^n + v_{i\uparrow}^{n*} c_{i\uparrow}^{-n\dagger}). \quad (11)$$

Here the index n ($-n$) represents the energy ε_n ($-\varepsilon_n$) of an eigenstate for the BdG equation (4). By making use of the partical-hole symmetry property, $u_{i\uparrow}^n = v_{i\uparrow}^{-n*}$ and $u_{i\downarrow}^n = -v_{i\downarrow}^{-n*}$, we can get

$$\gamma_n = \sum_i (v_{i\uparrow}^{-n} c_{i\uparrow}^n + u_{i\downarrow}^{-n} c_{i\downarrow}^{-n\dagger}) + (-v_{i\downarrow}^{-n} c_{i\downarrow}^n + u_{i\uparrow}^{-n} c_{i\uparrow}^{-n\dagger}) = \gamma_{-n}^\dagger. \quad (12)$$

The last expression indicates that the quasi-particle creating operator would behave as an annihilation operator if acting on the zero-energy state, satisfying the Majorana condition. It is therefore concluded that the Majorana fermions are readily fabricated/constructed with the zero-energy chiral edge modes.

One more point we would stress is that Majorana fermions have to appear in pair nonlocally. In the present case, Majorana zero-energy modes may develop at the opposite edges of the YBCO strip. It is accessible as the electron and hole wave functions associating with the lowest-energy state have an identical phase factor on one edge and a reverse phase factor at the opposite edge of the superconductor strip, as shown in fig. 2.

We take the lowest state as the zero-energy state and denote the eigenvector as $a = [u_{i\uparrow}^n, u_{i\downarrow}^n, v_{i\uparrow}^n, v_{i\downarrow}^n]$. According to the partical-hole symmetry, the vector

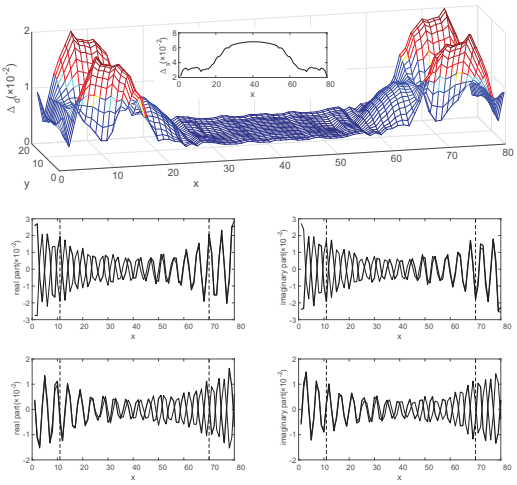

Fig. 3: (Color online) The superconductor order parameter distribution in a magnetic unit cell with two superconductive fluxons. Top panel: the d-wave superconductor order parameter, evaluated as $\Delta_d = (\Delta^A_{i+\vec{e}_x,i} + \Delta^A_{i-\vec{e}_x,i} - \Delta^A_{i,i+\vec{e}_y} - \Delta^A_{i,i-\vec{e}_y})/4$, with $\Delta^A_{ij} = \Delta_{ij}\exp[i(\pi/\phi_0)\int_{\vec{r}_i}^{(\vec{r}_i+\vec{r}_j)/2}\vec{\mathbf{A}}(\mathbf{r})\cdot \mathrm{d}\vec{\mathbf{r}}]$. The inset shows the s-wave order parameter $[\Delta_s = (\Delta^A_{i+\vec{e}_x,i} + \Delta^A_{i-\vec{e}_x,i} + \Delta^A_{i,i+\vec{e}_y} + \Delta^A_{i,i-\vec{e}_y})/4]$ as a function of x on the line $y = 0$ crossing the vortex cores. The spatial distribution of $u_\sigma(x)$ (thick line) and $v_\sigma(x)$ (thin line) along $y = 0$ for the up-spin band (middle panel) and for the down-spin band (bottom panel).

$b = [v^{n*}_{i\uparrow}, -v^{n*}_{i\downarrow}, u^{n*}_{i\uparrow}, -u^{n*}_{i\downarrow}]$ is also an eigenvector. To guarantee the vector base that satisfies the particle-hole symmetry, one can construct a vector c given by $c = \frac{\sqrt{2}}{2}(a + b)$, denoted as $[u^0_{i\uparrow}, u^0_{i\downarrow}, v^0_{i\uparrow}, v^0_{i\downarrow}]$. Apparently, the electron (hole) wave function $u^0_{i\uparrow(\downarrow)}(v^0_{i\uparrow(\downarrow)})$ has an identical spatial distribution as that of $u^n_{i\uparrow(\downarrow)}(v^n_{i\uparrow(\downarrow)})$. The Majorana fermion creation/annihilation operator may be constructed as below.

We examine what occurred on the left edge (labeled as 1). As electron and hole wave functions have opposite signs, that is, $u^0_{i1\uparrow} = -v^0_{i1\uparrow}$(see, fig. 2) the up-spin electron wave function $u^0_{i1\uparrow}$ has to a pure imaginary in order to satisfy the electron-hole symmetry constrain $u^0_{i1\uparrow} = v^{0*}_{i1\uparrow}$. For the down-spin band, $u^0_{i1\downarrow}$ is also a pure imaginary since $u^0_{i1\downarrow} = v^0_{i1\downarrow}$ (see, fig. 2) while $u^0_{i1\downarrow} = -v^{0*}_{i1\downarrow}$ (the particle-hole symmetry condition). On the same account, the electron wave function $u^0_{i2\uparrow}$ and $u^0_{i2\downarrow}$ are both real number on the right edge (labeled as 2). Therefore, the Bogoliubov quasi-particle operator in eq. (11) becomes $\gamma_{1\sigma} = i(c^{0\dagger}_{i1\sigma} - c^0_{i1\sigma})$, and $\gamma_{2\sigma} = (c^{0\dagger}_{i2\sigma} + c^0_{i2\sigma})$. Pairs of Majorana zero-energy modes are then generated with the quasi-particle operators $\gamma_{1\sigma}$ and $\gamma_{2\sigma}$ acting on $[u^0_{i\uparrow}, u^0_{i\downarrow}, v^0_{i\uparrow}, v^0_{i\downarrow}]$.

The MBSs in the vortices. – In this section, we showed that the Majorana edge modes may be manipulated with a normal magnetic field. We assume that a magnetic unit cell has dimension $40a \times 20a$, where a is the lattice constant. We discuss the case of two flux quanta in two magnetic unit cells. We make the open boundary condition in the x-direction and the periodic boundary condition in the y-direction. We diagonalize the model Hamiltonian by solving the BdG equation (4) self-consistently. Spatial distributions of the order parameters are shown in fig. 3 for an underdoped ($\bar{n} = 0.896$) YBCO superconductor. Remarkably, strip-like domains have developed. Close to the sample edges there are the d-wave dominant domains. Meanwhile, vortex cores locate at the center of the d-wave domains. In the middle region, however, an s-wave domain is found. We would point out that the s-wave domain would shrink to disappear when the doping level increases to or beyond the optimum doping region, say, the average electron number density $\bar{n} < 0.85$. These results suggest that an s-wave pairing state may coexist with the d-wave pairing state for the underdoped YBCO superconductor. Recent experiments on the underdoped $Bi_2Sr_2CaCu_2O_{8+\delta}$ superconducting film by Zhong *et al.* [22] also reported an analogous phenomenon.

Another noticeable phenomenon is that an identical phase or a π phase difference in the electron and hole wave functions for the zero-energy chiral edge state remains holding for only at the horizontal axis $y = 0$ (the line with the y-direction grid number $Ny = 10$) that crosses through the vortex cores. Due to a cylindrical symmetry of the vortex, the microscopic current has only an angular component. The relative phase difference in electron and hole wave functions for the edge states must have an exactly same value as that for the core state with zero energy, to guarantee no normal current on the edges at $y = 0$. The dashed lines intersecting with the horizontal axis marked the vortex core locations. Spatial variations of $u_\sigma(x, 0)$ and $v_\sigma(x, 0)$ as a function of the x variable are shown in the middle and bottom panels in fig. 3. Very interestingly, while the phases in the electron and hole wave functions are synchronized for one core state with zero energy it has a π phase different at another core state. Furthermore, the wave functions of the zero-energy core state have an exactly the same spatial distribution as that of the neighboring edge state. Thus, as described in eqs. (11) and (12), the Majorana particle creation and annihilation operators can be constructed with those zero-energy modes, for instance, either a pair of the zero-energy core state or one core state and the remote edge state.

The phase diagram with V_{so} *vs.* δ. – As discussed in previous sections, the spin-orbit coupling and Zeeman exchange field-induced conversion in the ground-state parity give a fundamental mechanism for the occurrences of the chiral edge state and the MBS. In practical settings, the exchange field can be included into the model Hamiltonian by depositing the high-T_c superconducting film on a magnetic substrate. The Rashba spin-orbit coupling is, however, more subtly, despite that a relatively strong surface Rashba-type spin-orbit coupling would be expected [23] by doping ions with different valances on the metallic Cu-O plane, which leads to the up-down symmetry violation [24]. Therefore, a discussion on the

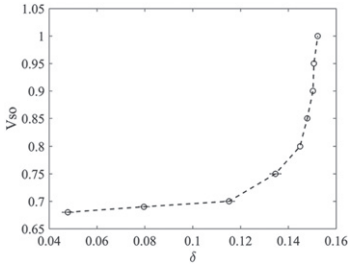

Fig. 4: (Color online) The phase diagram for the hole-doped YBCO superconductor. The parameters used are $T = 0$, $Nx = 80$, $Ny = 201$, $U = 3$, $V = 3$, and $h = 0.55$.

low-boundary value of the SO coupling that would support the chiral edge state becomes important. Figure 4 shows the phase diagram. The doping level δ is defined as $\delta = 1 - \bar{n}$, with $\bar{n}$ the average electron density. The dashed line is the phase boundary that separates the chiral edge state phase of nontrivial topology from the phase of trivial topology. It illustrates how the lowest SO amplitude required for the chiral edge state surviving would increase (exponentially) with the doping level. It would become unphysical large when the doping level is beyond the so-called optimum doping $\delta = 0.15$, the overdoped case. On the other hand, the chiral edge state is expected in the presence of a reasonable large SO coupling for the underdoped sample. This is because the topology of the Fermi surface changes dramatically with the doping level in copper-oxide high-T_c superconductors. The normal phase itself is a Fermi liquid for the overdoped sample, but a non-Fermi liquid for the underdoped samples.

Conclusions. – In conclusion, we have investigated the chiral edge states and Majorana fermions in the hole-doped YBCO mesoscopic strip. Coexistences and competitions of different orderings provided fundamental and intrinsic processes for the state with nontrivial topology in the system. Spin-orbit coupling and Zeeman field assistant conversions between states with different symmetry have been discussed. The Majorana zero-energy mode is predicted, which is most likely to occur in the underdoped samples. It is worthwhile to mention that there were no Majorana zero-energy modes in edges or vortex for a s-wave superconductor in the absence of the spin-orbit interaction and the Zeeman field. For a p-wave superconductor, however, there are indeed Majorana zero modes in a vortex, as studied by several research groups [14,25] and 1 chiral Majorana-Weyl mode per edge (central charge $c = 1/2$). This is related to the Ising anyon [26]. In addition, for a $(d + id)$-wave superconductor, the gap-closing condition does not depend on the amplitude of the pairing gap. Interestingly, with a weak Zeeman field less than the gap amplitude, the gap can also close and the topological phase transition [27] occurs, this will be investigated in our future work.

* * *

We are grateful to L.-F. Zhang for fruitful discussions. This work was supported by National Natural Science Foundation of China under Grants No. 61571277 and No. 61771298.

REFERENCES

[1] Hasan M. Z. and Kane C. L., *Rev. Mod. Phys.*, **82** (2010) 3045.
[2] Qi X.-L. and Zhang S.-C., *Rev. Mod. Phys.*, **83** (2011) 1057.
[3] Majorana E., *Nuovo Cimento*, **14** (1937) 171.
[4] Stern A., *Nature (London)*, **464** (2010) 187.
[5] Nayak C., Simon S. H., Stern A., Freedman M. and Das Sarma S., *Rev. Mod. Phys.*, **80** (2008) 1083.
[6] Moore G. and Read N., *Nucl. Phys. B*, **360** (1991) 362.
[7] Read N. and Green D., *Phys. Rev. B*, **61** (2000) 10267.
[8] Bonderson P., Kitaev A. and Shtengel K., *Phys. Rev. Lett.*, **96** (2006) 016803.
[9] Clarke D. J., Alicea J. and Shtengel K., *Nat. Commun.*, **4** (2013) 1348.
[10] Ivanov D. A., *Phys. Rev. Lett.*, **86** (2001) 268.
[11] Tewari S., Das Sarma S. and Lee D. H., *Phys. Rev. Lett.*, **99** (2007) 037001.
[12] Gurarie V. and Radzihovsky L., *Phys. Rev. B*, **75** (2007) 212509.
[13] Bolech C. J. and Demler E., *Phys. Rev. Lett.*, **98** (2007) 237002.
[14] Lou Y. F., Wen L., Zha G. Q. and Zhou S. P., *Sci. Rep.*, **7** (2017) 9871.
[15] Tewari S., Das Sarma S., Nayak C., Zhang C. and Zoller P., *Phys. Rev. Lett.*, **98** (2007) 010506.
[16] Zhang C., Tewari S., Lutchyn R. M. and Das Sarma S., *Phys. Rev. Lett.*, **101** (2008) 160401.
[17] Jiang L., Kitagawa T., Alicea J., Akhmerov A. R., Pekker D., Refael G., Cirac J. I., Demler E., Lukin M. D. and Zoller P., *Phys. Rev. Lett.*, **106** (2011) 220402.
[18] Sato M., Takahashi Y. and Fujimoto S., *Phys. Rev. Lett.*, **103** (2009) 020401.
[19] Bednorz J. G. and Mller K. A., *Z. Phys. B*, **64** (1986) 189.
[20] Tsuei C. C. and Kirtley J. R., *Rev. Mod. Phys.*, **72** (2000) 969.
[21] Meng H., Zhao H. W., Zhang L. f., Shi L. M., Zha G. Q. and Zhou S. P., *EPL*, **88** (2009) 17005.
[22] Zhong Y., Wang Y., Han S., Lv Y. F., Wang W. L., Zhang D., Ding H., Zhang Yi. M., Wang L. L., He K., Zhong R. D., Schneeloch J. A., Gu G. D., Song C. L., Ma X. C. and Xue Q. K., *Sci. Bull.*, **61** (2016) 1239.
[23] Silsbee R. H., *J. Phys.: Condens. Matter*, **16** (2004) R179.
[24] Edelstein V. M., *Phys. Rev. Lett.*, **75** (1995) 2004.
[25] Matsumoto M. and Heeb R., *Phys. Rev. B*, **65** (2001) 014504.
[26] Putrov P., Wang J. and Yau S.-T., *Ann. Phys. (N.Y.)*, **384** (2017) 254.
[27] Sato M., Takahashi Y. and Fujimoto S., *Phys. Rev. B*, **82** (2010) 134521.